Journal of
Vibration and Control

Design and Validation of a Hardware-In-the-Loop Test Bench for Evaluating the Performance of an Active Mass Damper

Journal:	*Journal of Vibration and Control*
Manuscript ID	JVC-22-0223.R1
Manuscript Type:	Original Manuscript
Date Submitted by the Author:	n/a
Complete List of Authors:	Rosti, Matteo; ISAAC Antisismica s.r.l. Cii, Stefano; ISAAC Antisismica s.r.l. Bussini, Alberto; ISAAC Antisismica s.r.l. Calvi, Paolo; University of Washington, Department of Civil and Environmental Engineering Ripamonti, Francesco; Politecnico di Milano, Meccanica
Keywords:	Active Mass Damper, Active vibration control, Hardware-In-the-Loop, Sky-Hook algorithm, Triple Variable Control, Seismic protection
Please select up to 5 subject areas that best reflect the content of your manuscript:	Structural control/vibration mitigation, Earthquake engineering, Identification, Control theory
Abstract:	The purpose of this study is to propose an innovative solution for evaluating the performance of a full-scale Active Mass Damper (AMD). The AMD adopted is a custom hydraulic actuator, developed for active control of existing buildings against earthquakes. For vibration control a Sky-Hook algorithm was implemented. Its characteristics ensure good robustness, which is fundamental in structural engineering since buildings are subjected to significant variation in dynamic properties in presence of damage or ambient conditions. A Hardware-In-the-Loop (HIL) test bench was specifically designed to simulate the actual working condition of the anti-seismic system. The HIL setup consists of a shaking table moved by a hydraulic actuator in accordance with the roof's displacement, evaluated using a structural numerical model of the building to which the AMD is fixed. The presence of two distinct active systems (HIL and AMD) could generate control issues, therefore, a Triple Variable Control logic was introduced to reduce the interaction delay. The effectiveness of the proposed AMD is validated comparing the roof's displacement in an uncontrolled structure with that in a controlled one. Also, the robustness of the control algorithm was verified using a non-linear structural model and applying seismic excitation at different intensities.

Design and Validation of a Hardware-In-the-Loop Test Bench for Evaluating the Performance of an Active Mass Damper

Matteo Rosti[1], Stefano Cii[1], Alberto Bussini[1], Paolo M. Calvi[2] and Francesco Ripamonti[3]

[1]ISAAC Antisismica S.r.l., Via Magolfa 27, 20143 Milan, Italy

[2]Department of Civil and Environmental Engineering, University of Washington, Seattle (WA, USA)

[3]Department of Mechanical Engineering, Politecnico di Milano, Via La Masa 1, 20156 Milan, Italy

Abstract

The purpose of this study is to propose an innovative solution for evaluating the performance of a full-scale Active Mass Damper (AMD). The AMD adopted is a custom hydraulic actuator, developed for active control of existing buildings against earthquakes. For vibration control a Sky-Hook algorithm was implemented. Its characteristics ensure good robustness, which is fundamental in structural engineering since buildings are subjected to significant variation in dynamic properties in presence of damage or ambient conditions. A Hardware-In-the-Loop (HIL) test bench was specifically designed to simulate the actual working condition of the anti-seismic system. The HIL setup consists of a shaking table moved by a hydraulic actuator in accordance with the roof's displacement, evaluated using a structural numerical model of the building to which the AMD is fixed. The presence of two distinct active systems (HIL and AMD) could generate control issues, therefore, a Triple Variable Control logic was introduced to reduce the interaction delay. The effectiveness of the proposed AMD is validated comparing the roof's displacement in an uncontrolled structure with that in a controlled one. Also, the robustness of the control algorithm was verified using a non-linear structural model and applying seismic excitation at different intensities.

Keywords: Active Mass Damper, Active vibration control, Hardware-In-the-Loop, Sky-Hook algorithm, Triple Variable Control

1 Introduction

In recent decades, the scientific community has focused on the vibration of structural buildings (Beards CF, 1996; Fahy F and Gardonio P, 2007) and the problem of reducing it using passive or active systems. There are different kinds of sources that

induce vibrations in structures, but the most dangerous one is an earthquake due to its detrimental effects on human health and infrastructures (Bolt BA, 2020).

The challenging task of seismic hazard mitigation was traditionally approached by designing structures with sufficient strength capacity and the ability to deform in a ductile manner. However, very often, the traditional seismic-resistant methods cannot meet the design requirements for new buildings. Thus, the Active Vibration Control (AVC), already adopted in the aerospace and mechanical industries, is becoming an increasingly attractive solution in civil structural engineering as well (Cheng FY et al., 2008; Septimiu et al., 2005). The structural vibration control consists of integrating energy dissipation devices in the system, that are able to effectively keep the response under earthquake, strong wind or other dynamic disturbances within the allowable range (Aiqun Li, 2020). Over the years, technological progress has made it possible to create new and cheaper anti-seismic devices. The different systems and technologies used can be grouped into four main categories: isolation, passive, active and semi-active systems.

~~The technologies most often adopted are the isolation and passive systems. The former consist of applying low lateral stiffness material to the buildings' foundations in order to achieve a flexible base, able to filter out high frequencies from the ground motion (Patil and Reddy, 2012; Calvi Paolo and Calvi Gian Michele, 2018). On the other hand, the passive energy dissipation systems are mechanical elements, like springs and dampers, that reduce the structural response through partial dissipation of the input energy. Typical passive systems are Tuned Mass Dampers (Gutierrez SM and Adeli H, 2013) and Tuned Liquid Dampers (Tait MJ et al., 2008).~~

~~The~~

The technologies most often adopted are the isolation and passive systems (Patil and Reddy, 2012; Calvi P and Calvi GM, 2018; Gutierrez SM and Adeli H, 2013; Tait MJ et al., 2008). However, the recent idea of creating smart buildings (Snoonian D, 2003) by adopting sensor and automation systems, allowed the use of semi-active and active control devices to spread. The semi-active systems are the evolution of passive technology as they incorporate adaptive features, powered by a small external power source, to improve the magnitude of the control force (Ning D et al., 2020). Active control systems are actuators that generate a force directly on the building; for this reason, they require a high external power source and a proper control algorithm.

Active Mass Dampers (AMDs) are an example of this technology. They consist of an inertial mass moved by an electro-mechanical or electro-hydraulic actuator in order to generate the control force (typically on the building's roof where its effect is maximised). Although the AMDs have been studied since the 1980s they have been implemented in a small number of structures (Yamamoto M et al., 2001). The main reasons are the high design and test cost of the AMD for each building application.

However, not only does the high design costs often lead to structural engineers opting for other cheaper technologies, but the difficulties in evaluating the real performance of the AMD during the design phase are also a significant obstacle for this technology to flourish. The difficulties in realising a full-scale test bench mean

that usually performance levels are estimated by means of numerical simulations or, in very few cases, a small-scale model.

The most complex solution implemented was a real-time hybrid simulation (Xu H et al., 2014), in which the AMD was a full-scale subsystem and the structure's dynamics were reproduced numerically. Even though this method makes it possible to assess the actuator's functionality, it is not able to evaluate the impact of structural interactions and disturbances on the device.

In this context, this work proposes an innovative way to overcome these limits, by using a HIL test bench. It is composed of a shaking table that simulates the structure's dynamics and, upon it, the AMD. In this manner, it is possible to test not only the control system, but also its interaction with the building and the sensors' noise rejection in operating conditions. The AMD used as a reference is a newly developed hydraulic actuator: a modular device that, according to the required vibration reduction, can be integrated in a multi-device system able to work simultaneously to control the building.

The article is organised as follows. First, the AMD technology is introduced, with particular focus on the actuator proposed for the tests and its control algorithm. Afterwards, the HIL test bench is described, defining the approach used to evaluate the building's dynamic response. Finally, the experimental results are illustrated, validating the system's performance and robustness.

2 The Active Mass Dampers

The major advantages of AMDs compared to other traditional technologies for the vibration suppression in large civil structures are reiterated briefly. Compared to isolations systems or other passive systems, such as structural reinforcements, the AMD can be installed without the need of an invasive intervention, and the related difficulties, on existent structures.

~~A similar kind of intervention, that can easily be applied to existing structures, is the so-called Tuned Mass Damper. Like AMDs the TMDs' working principle is also based on a moving mass able to apply inertial forces on the structure. Unfortunately, TMDs are passive systems and have to be designed ad-hoc for each application. Moreover, existing TMDs usually require the use of heavy weights. On the other hand, the AMDs are more versatile solutions, since active systems can be adapted to different structures, and much smaller masses can be used to obtain the same dissipating forces. Moreover, while the TMDs can only work efficiently on the structure's first mode, the AMDs can act over a wider frequency range. At the same time, the main drawback of AMD systems is the higher level of complexity and higher maintenance requirements.~~

In literature, one of the first applications of an AMD to an existing structure dates back to 2001. (Ikeda et al., 2001). In their work, Ikeda et al. applied two hydraulic AMDs to an 11-storey building. The device was used to reduce vibrations on the building introduced by both wind and seismic actions. In-the-field data was sampled and demonstrated the effectiveness of the device in increasing comfort in case of

strong wind (reducing the oscillation amplitude). Some earthquakes also happened during the period in which the AMD was installed, demonstrating the system's effectiveness in increasing structural damping of the controlled structure.

Some years later Y. Matsumoto et al. (Matsumoto Y et al., 2004) considered the possibility of installing a smaller AMD, actuated by means of an electrical motor with a ball-screw transmission and a moving mass of less than 200 kg, on 3-storey buildings, to reduce traffic-induced vibrations. For both the systems mentioned, a Linear Quadratic Regulator (LQR) was adopted as the control logic.

However, in relation to vibration control of civil structures, a different solution was also proposed by Japanese researchers (Miyazaki M et al., 2004). The authors demonstrate the feasibility of applying a small AMD to 3-storey slender buildings, adopting a Direct Velocity Feed-Back (DVFB) control logic to produce a skyhook effect on the building. The strength of the method proposed is the robustness of the control logic that does not require full knowledge of the building's dynamic model.

2.1 The ISAAC I-Pro 1

More recently, the Italian startup ISAAC Antisismica S.r.l. proposed a new AMD for vibration suppression in civil structures. It is the I-Pro 1 model that was chosen as a test case in this work. A double-acting hydraulic actuator is adopted in order to minimise the dimensions of the inertial actuator. The piston rod is considered to be the fixed part, while the tube cylinder, together with the hydraulic components, are the inertial mass. The hydraulic actuator is moved by high-pressure oil (up to 320 bar, with nominal pressure of 280 bar) able to generate a nominal linear force equal to 158 kN (peak force of 220 kN).

The oil flow and, consequently, the force application direction is governed by a proportional solenoid valve. The valve is controlled by its own electronics and its position defines the motion of the cylinder tube.

The high-pressure oil is stored in a 50 lit tank, thanks to a pre-compressed fluid (nitrogen) which keeps the operating pressure within a certain range (from a minimum of 180 bar up to 280 bar). The tank is refilled by a 1.5 kW volumetric pump. The different components of the hydraulic actuator (tank, piston, valve etc.) form the moving mass of the AMD and weigh about 2200 kg.

Two kinds of sensors are used to control the AMD: a LVDT sensor for position control of the moving mass and MEMS accelerometers for evaluating the actual force generated by the device.

The position control logic of the AMD is implemented on the Slave PLC (RT3-SM) which regulates the actuator's motion. The control force and vibration algorithm is implemented on the Master PLC (Mobile real-time Speedgoat).

2.2 The I-Pro 1 Control Algorithm

In order to properly consider its interaction with the HIL test bench, a brief description of the I-Pro 1 control algorithm is summarised here.

Figure 1 shows the overall control algorithm, that receives the measured acceleration of the structure's roof as input, and returns the spool command to move the AMD. It consists of three main logic blocks: position control, force control and vibration control.

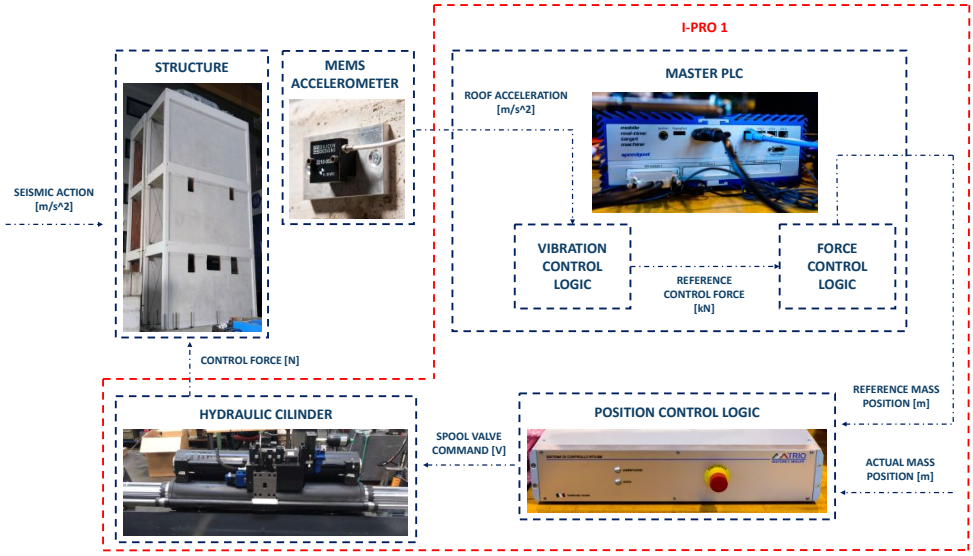

Figure 1. Block diagram of the ISAAC I-PRO1 Control Algorithm.

2.2.1 Position Control Logic

To control the position of the inertial mass, a PID logic has been implemented that takes the actuator's reference and actual positions as input, and gives the spool valve command signal as output.

The parameters were tuned considering the following rules:

- The proportional variable (P) should be sufficiently high to reduce the stick-slip phenomenon generated by the friction forces at low frequencies
- The integral coefficient (I) should allow good reference tracking
- The derivative variable (D) should grant a reduction in delay at high frequencies, without elevated overshooting
- The control bandwidth should guarantee a frequency range of at least 0-10 Hz.

Besides the PID controller, a notch filter of around 11 Hz was implemented to mitigate the effect of instability of the oil column, a characteristic phenomenon of the hydraulic actuators. Figure 2 shows the closed-loop system's Frequency Response Function (FRF) between the actual and the reference position, generated in an experimental sweep test from 0.5 to 20 Hz. The position control obtained has a frequency bandwidth of 0-11 Hz and an amplification magnitude lower than 9 dB.

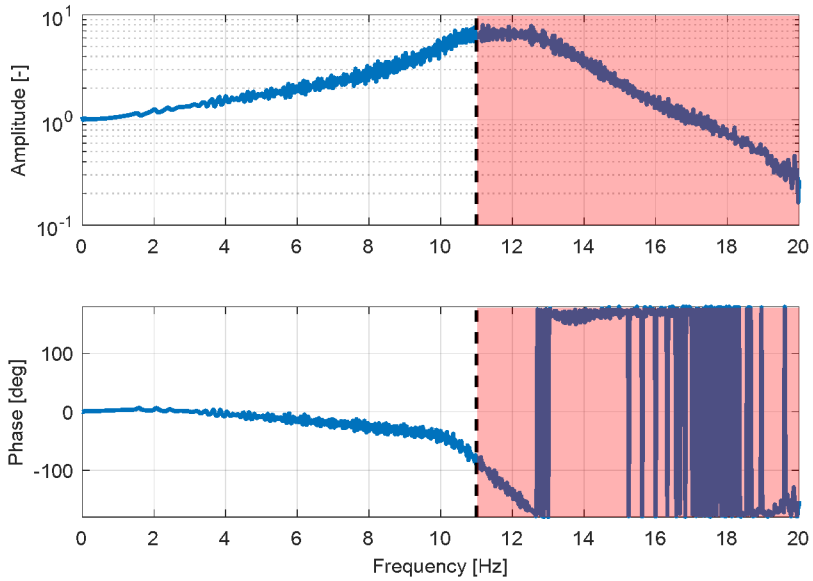

Figure 2. The position control logic: Frequency Response Function (FRF) between actual and reference position.

2.2.2 Force Control Logic

The mass movement produces an inertial force that is transmitted to the roof. The reference force required is computed by a vibration control logic.

Dealing with inertial actuators, the target force F_c is obtained as

$$F_c = -ma = -m\ddot{x} \tag{1}$$

where m is the AMD moving mass and $\ddot{x}$ is its absolute acceleration. Therefore, the force is processed as a reference acceleration, inverting equation (1) and knowing the value of m. Finally, from the acceleration, the mass position can be calculated.

These passages are implemented through an algorithm based on a Three Variable Control (TVC) logic, which gives higher performance than a common double integration and double filtering (DIDF) approach. Indeed, the DIDF approach's performance is limited, at high frequencies, by the PID ones and, at low frequencies, by the high-pass filter, in order to remove the integration divergence.

Different implementations and tuning of the TVC logic are reported in literature (Shen G et al., 2011; Yu T et al., 2015). Generally, the TVC is composed of three main components: signal generator, TVC feed-forward and TVC feed-back. In this application, in order to guarantee the control's robustness, thus avoiding any potential instability, in the Force control algorithm only the signal generator and the TVC feed-forward were implemented. The TVC transfer function adopted is defined by

$$TF_{TVC} = K_0 \frac{K_{ar} \cdot s^2 + K_{vr} \cdot s + K_{dr}}{s^2 + v_0 \cdot s + d_0} \tag{2}$$

Looking at TF_{TVC} formulation, it can be noticed that 6 parameters must be tuned:

- K_{ar}, the feed-forward acceleration gain

- K_{vr}, the feed-forward velocity gain
- K_{dr}, the feed-forward position gain
- K_0, the signal generator acceleration gain
- v_0, the signal generator velocity gain
- d_0, the signal generator position gain.

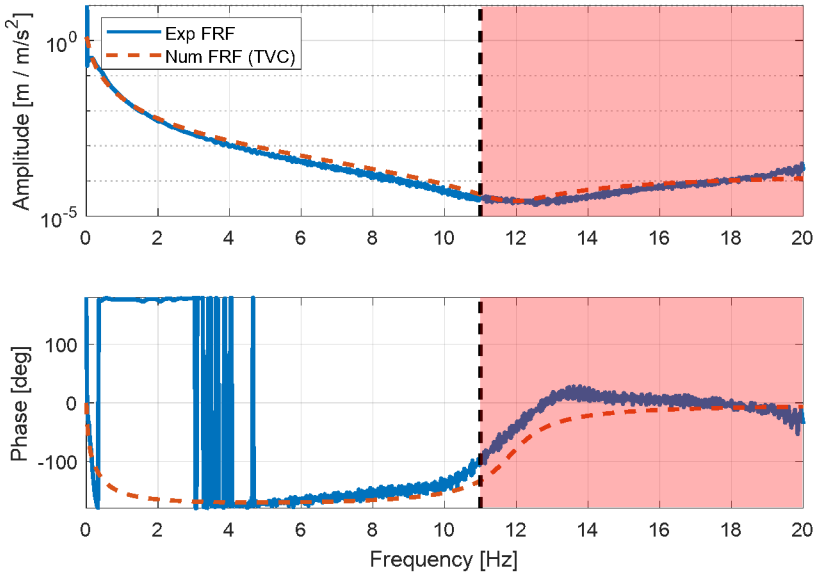

Figure 3. The force control logic: comparison between the experimental and the numerical-TVC FRF (between acceleration and position of the AMD moving mass).

These parameters were tuned in order to match the FRF between the relative mass reference position and the mass acceleration, measured experimentally by means of a sweep test within the frequency range of interest (Figure 3).

2.2.3 Vibration Control Logic

The core of an active mass damper is the Vibration Control algorithm which defines the target force that should be generated on the structure to obtain a desired vibration suppression. Many control logics can be found, in literature, such as the neural network controllers (Yang SM et al., 2006; Madan Alok, 2005), the fuzzy logic together with the PID controller (Thenozhi and Yu, 2015; Guclu and Yazici, 2007) or the sliding mode (Rahmi, 2006; Yang JN et al., 1997) and in general they can be classified in two main groups: Model Based and Non-model Based controllers.

Model Based algorithms need a dynamic model of the controlled system and they are usually perform best (Sakizlis V et al., 2004). Nevertheless, the definition of a structural dynamic model is difficult and computationally cumbersome, especially in real-time. For this reason, the model is usually made offline and is not adaptive. Consequently, there is a significant reduction in robustness in the presence of structural damage, which leads to a better performing non-model based controller being preferred (Bui H-L et al., 2017; Jue Wang et al., 2019).

In this application the main criteria used to choose the proper algorithm were the performance and robustness. Thus, a Direct Velocity Feed-back control, which does not need a building model to be created, was implemented. This control architecture is also commonly known as Sky-Hook. Indeed, the overall effect of the AMD on the structure can be seen as an equivalent damper (well-known as "dissipative towers"). The algorithm defines a control force proportional to the velocity of the point at which the actuator is installed (e.g. the building rooftop velocity in relation to the ground, called $\dot{x}_{roof}$), the equation for which can be written as

$$F_{control} = -G \cdot \dot{x}_{roof} \tag{3}$$

where G is the equivalent damping coefficient. A description of the G tuning strategy will be presented in the Section 4.1, accounting for the performances of complete system. Indeed, previous works proved the good performance of this control algorithm (Miyazaki M et al., 2004), but some deeper investigations show that the closed-loop system's stability is not guaranteed when the actuator is unable to follow the reference force (Ubertini F et al., 2015). Moreover, since the control parameter G can be freely set by the designer it is crucially important that the optimal value be chosen correctly. In fact, a low value of G leads to poor performance of the AMD, while a value of G that is too high can lead to dynamic instability of the system. For all these reasons, the dynamic performance of the AMD must be proven in accordance with the gain G selected and the controlled building's dynamics. It is worth mentioning that the same conclusions are valid also if we adopted other Vibration Control logics, such as the Model Based algorithms previously introduced, especially considering that for these logics the stability analysis may represent an even more critical aspect.

3 The Hardware-In-the-Loop test bench

Hardware-In-the-Loop (HIL) simulation is a technique for performing system tests in a comprehensive, cost-effective, and repeatable manner. It consists of a mix of numerical model and real devices, which interact with each other to simulate the working condition of the tested components in real-time. In this application, the structural dynamic was simulated numerically and the outputs were used to move a shaking table in accordance with the roof's displacement. Figure 4 shows the layout of the HIL test bench. The shaking table consists of hollow beams welded together to form two frames; the first (blue) is fixed to the ground, while the second (white) is moved by a MTS hydraulic actuator (mod. 244.31) which can generate a force of up to 250 kN with a nominal flow rate of 140 l/min and a maximum displacement of ±125 mm. The shaking table has been designed to support the AMD static vertical load (40 kN) and the dynamic longitudinal load (220 kN). Moreover, its first resonance frequency is set above the upper limit of the bandwidth of AMD control logic (see Figure 2 and Figure 3).

The AMD is rigidly mounted on the moving frame of the shaking table and the control force generated is estimated using accelerometric sensors mounted on the

AMD cylinder tube, as previously described in section 2.1. ~~Figure 4 shows the layout of the HIL test bench.~~ The complete list of sensors installed on the HIL test bench is shown in Table 1.

Table 1 – List of sensors installed on the HIL test bench

Sensor	Model	Location	Function
Accelerometer	SDI 2210-010	AMD Moving Mass	Measure the absolute acceleration of the moving mass: used to calculate the inertial force generated by the AMD
LVDT	Temposonics RP5SA1200M01D701S1011B8	AMD Moving Mass	Measure the position of the mass: used to close the feed-back loop of the Position Control Logic (see Section 2.2.1)
Accelerometer	SDI 2210-002	Shaking table	Measure the absolute acceleration of the shaking table: used to estimate (through numerical integration) the velocity and position of the moving part (white), simulating the roof motion

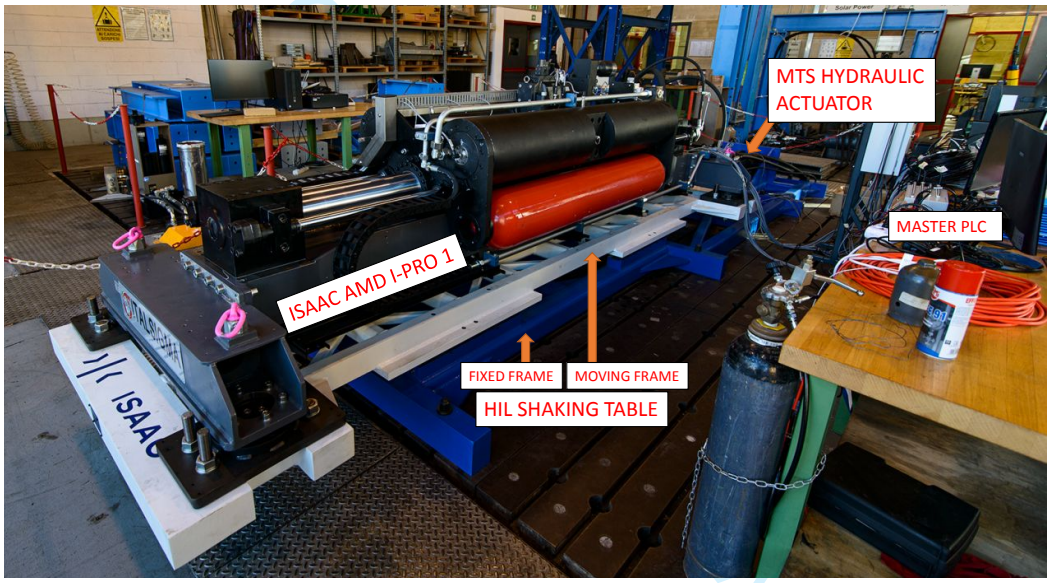

Figure 4. Overall view of the physical HIL system.

The overall working diagram of the AMD system presented in Figure 1 was adopted to retrieve the functional scheme of the HIL architecture, shown in Figure 5.
The inputs, in the form of the seismic action and dynamic response of the structural model, are shown in green since their behaviour is simulated numerically. The shaking table and the AMD are shown in red since they are physically present in the test bench.

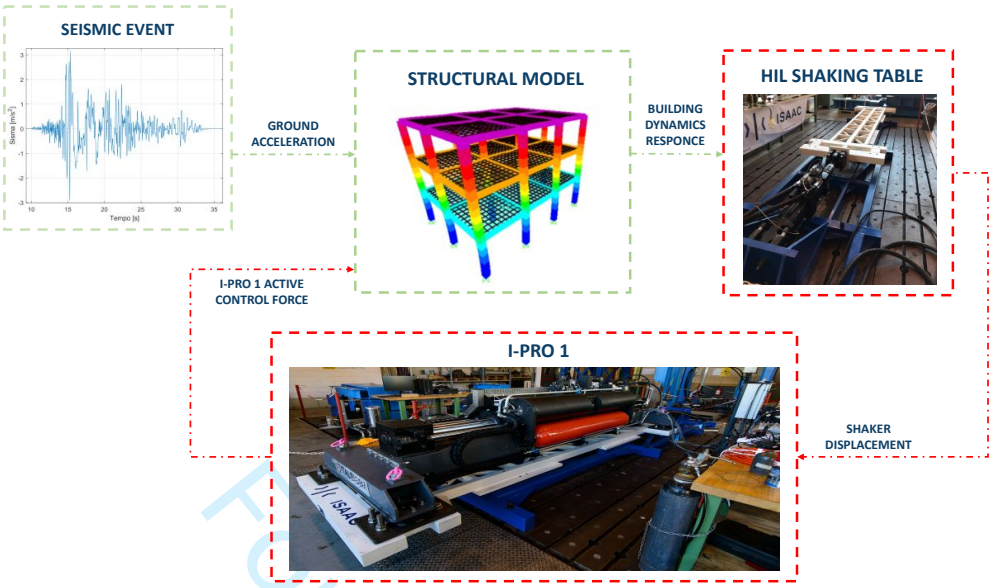

Figure 5. Hardware in the Loop (HIL) scheme: physical (red lines) and virtual (green lines) signals.

The HIL test bench loop is closed at a frequency of 1 kHz, which guarantees high dynamic performance and ideal behaviour, avoiding numerical instabilities. The following steps were run at each time interval:

1. Evaluating the earthquake input at the current time step and the force generated by the AMD at the previous step
2. Computing the system's states from the structural model
3. Moving the shaking table according to the current response of the building's roof
4. Acquiring the table's acceleration using physical transducers (MEMS accelerometers ID/2210-002 Silicon Design ±2 g)
5. Controlling the AMD according to the reference position, adopting the control logic described in section 2
6. Measuring the real active force generated by the AMD and giving it as feedback to the rooftop node where the AMD is applied in the structural model.

The whole procedure was run cyclically at each time step integration, until the whole earthquake time history was simulated.

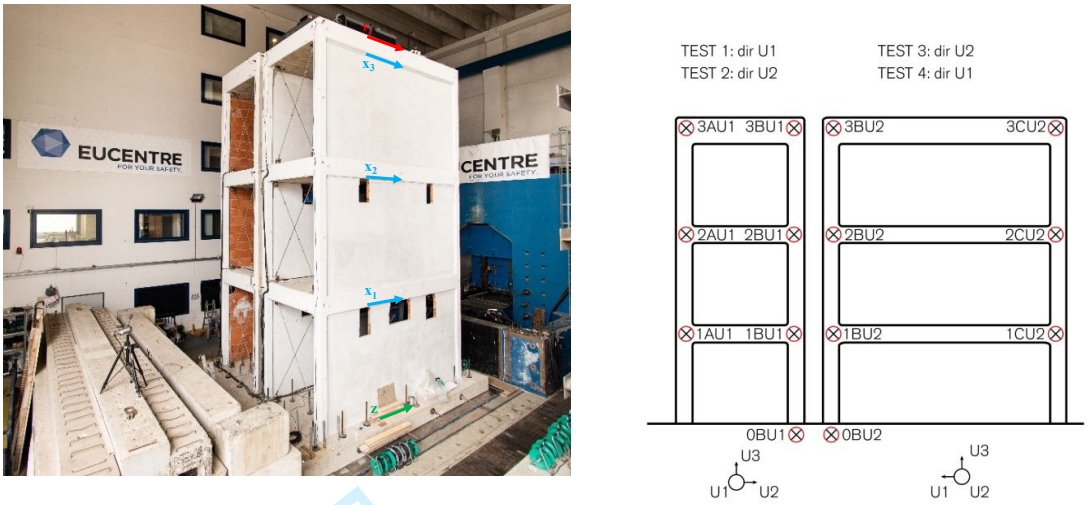

(a) (b)

Figure 6. The full scale real three-storey building placed in the EUCENTRE Laboratory (a) and Experimental Modal Analysis (EMA) on the 3-story RC building: layout of the sensors and summary of the test performed (b).

3.1 The case study: 3-story RC building

Figure 6a shows the real three-storey Reinforced Concrete (RC) building used as a reference test case. It has a height of 9.3 m and floor area of 5x2.1 m. The building is located in the EUCENTRE laboratory, on the 1D shaking table, in order to be used for future tests using a full-scale structure.

Before presenting the building's numerical model, the typical behaviour of a reinforced concrete building with masonry infills subjected to a seismic event is described.

The presence of non-structural elements, such as masonry infills in the structure, produces a strong increment in the natural frequencies and a reduction in the damping in the linear range compared to the hypothesis of a bare-frame structure. During the seismic event, these non-structural elements are typically the first that are subjected to damage, thus implying a reduction in the stiffness of the structure and the appearance of a non-linear dissipation phenomenon due to hysteresis. The level of damage of non-structural elements can reach the point at which the masonry infills collapse completely, thus equivalent to a bare-frame of the structure in which the stiffness is due only to the reinforced concrete frame. Lastly, due to further damage to these structural elements, the stiffness can reduce even more, implying critical states and potential collapse of the building.

Starting from these considerations, the idea was to define a simple model able to capture the non-linear phenomena in order to correctly simulate the building's behaviour during the whole seismic event. Thus, the structure was modelled by means of a non-linear lumped-elements system described by a second Order Differential Equation (ODE)

$$[M_{FF}]\ddot{\boldsymbol{x}} + [C_{FF}(\boldsymbol{x})]\dot{\boldsymbol{x}} + [K_{FF}(\boldsymbol{x})]\boldsymbol{x} = [\Lambda_C]F_C - [M_{FC}]\ddot{\boldsymbol{z}} \quad (4)$$

where the stiffness K_{FF} and the damping C_{FF} matrices were initially tuned according to an Experimental Modal Analysis (EMA) carried out on the real structure with masonry infills. The EMA technique was also used to obtain the dynamic characteristics of the bare-frame (during the construction stage) in order to validate the capabilities of the model to correctly describe the non-linear behaviour of the structure.

~~The EMA was performed by installing a 1.5 kg linear vibrodine on the structure being tested together with piezoelectric accelerometers (PCB 393B12 ±0.5 g). The structure's FRFs were obtained from the ratio between the acquired acceleration at the different measurement nodes and the input dynamic force. Finally, the dynamic experimental model of the structure (valid only in the hypothesis of small vibrations) was extracted using proper post-processing algorithms such as the PolyMAX technique (Figure 7).~~

The EMA was performed by installing a 1.5 kg linear vibrodine on the building roof, generating a harmonic excitation of approximately 20 N, in both the U1 and U2 directions (Figure 6b). The structure vibration has been measured with 7 piezoelectric accelerometers (PCB 393B12 ±0.5 g). We have performed four tests with different layouts classified as "xxUy", where xx is the measuring position while y is the forcing direction.

Then, all the data have been processed to evaluate the structure FRFs between the acceleration at the different measurement nodes and the input force on the roof (transfer inertances). The dynamic model, both for Infilled and Bare-Frame structure, was estimated using the PolyMAX technique (Figure 7). Finally, the transition from Infilled to Bare-Frame state was obtained with a tuned Push-Over curve, implemented inside the stiffness $[K_{FF}(\boldsymbol{x})]$ matrix. This curve reduces the stiffness accordingly with the maximum inter-story drift reached at a given time step. More information about the Push-Over curve and the masonry infills damage modeling strategy can be found in literature (Hak S et al., 2012; Cavaleri L, 2014).

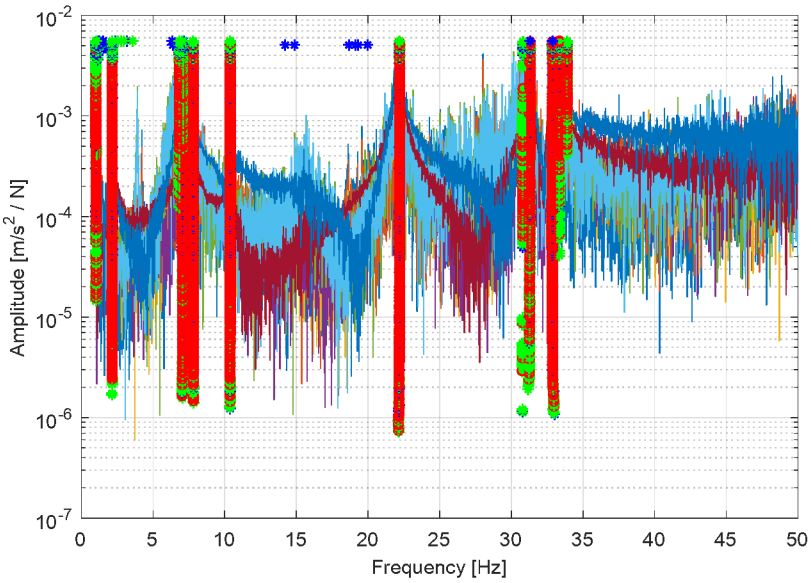

Figure 7. Example of PolyMAX Stability diagram calculated during the Experimental Modal Analysis (EMA) on the fully-infilled structure. FRFs between the accelerations measured at different points of the structure and the force of the vibrodine placed on the top floor.

In Table 2 the dynamic properties of the structural model are shown, for both the fully-infilled condition and for the bare-frame structure.

Table 2. Dynamic properties of the structure for two boundary conditions: Fully infilled and bare-frame structure

Property	Fully-infilled structure	Bare-frame structure
w_1	7.83 Hz	2.07 Hz
w_2	23.47 Hz	5.83 Hz
w_3	42.47 Hz	8.56 Hz
ξ_1	2 %	5 %

As regards the reference ground action, the acceleration time history recorded in Irpinia (Italy) during the 1980 earthquake was applied. It was the strongest earthquake ever recorded in Italy with a Magnitude (ML) of 6.9 and a recorded Peak Ground Acceleration (PGA) of 0.32g. During the tests, the earthquake amplitude was scaled with different multiplying factors to simulate different input intensity and evaluate the AMD's performance in different operating conditions.

The numerical simulation was run on a real-time computation device which interacted with the AMD via an I/O channel board.

3.2 The HIL Controller Design

Because the system is composed of two independent active control systems (the I-PRO 1 and the shaking table Figure 5), particular attention must be paid to the stability of the overall control loop. Indeed, the presence of two active devices could generate interaction lags which lead to instability.

In the overall system there are three main sources of delays:

1. Actual control force generation
2. Actual control force evaluation
3. Shaking table motion

The first is due to the AMD's dynamics that induce alteration of the reference in amplitude and phase. This phenomenon is inherent to the actuator and cannot be eliminated.

As concerns the second source, it does not exist in real working conditions for practical application to buildings, as there is no need to evaluate the actual control force. The force generated by the AMD instantaneously interacts with the structure as a whole continuous physical phenomenon. In the HIL, instead, the structure's dynamics is numerically simulated and, thus, the control action must be calculated. This delay is generated by the sensors used to evaluate the moving mass acceleration, and the clock frequency of the real-time computational device. It can be reduced by increasing the simulation frequency, with a significant drawback in that the computational process becomes cumbersome.

Finally, we have to consider the shaking table dynamics that, like for the AMD, introduced a delay. Again, this lag is not present in real working conditions, because the roof's dynamics is already considered in the real building system. This delay can be reduced thanks to the use of high-performance actuators and proper control algorithms aimed at improving the shaking table's acceleration response, which is used as feedback for the AMD control logics too. By considering all these issues, it is clear that a simple simulation of the building's behaviour, even without the influence of a real control force, can lead to instability. This situation is a serious concern in the world of HIL simulations and needs to be avoided. In order to achieve this goal and to reduce the computational efforts and the test bench cost, the TVC algorithm, tuned with the methodology previously described in section 2 for the AMD force control logic, was also implemented for the control of the HIL table.

4 Results and Discussion

The first purpose of this work is to demonstrate the performance of the HIL test bench as an innovative solution for investigating the AMD's behaviour, and so its capability to replicate the vibration of a reference building shaken by an earthquake. Thus, we started simulating the uncontrolled structure condition: the shaking table's capability to follow the correct reference signal was checked while the AMD was kept inactive.

For this test, the Irpinia earthquake was scaled down by a factor ~~of~~ ranged from 0.1 to 0.4, due to the oleo-dynamic limitation of the MTS actuator. Therefore, the ground excitation has a PGA of 0.128g, a magnitude close to half the intensity of the seismic event that occurred in Italy. Tracking of the shaking table's performance is shown in Figure 8 for the maximum operating condition (40% of the Irpinia earthquake), while Table 3 reports the comparison between the reference and actual displacement for different tests. A very good match and repeatability between the

reference signal, generated by the numerical model in real-time, and the actual shaking table displacement, measured by the sensor, can be observed.

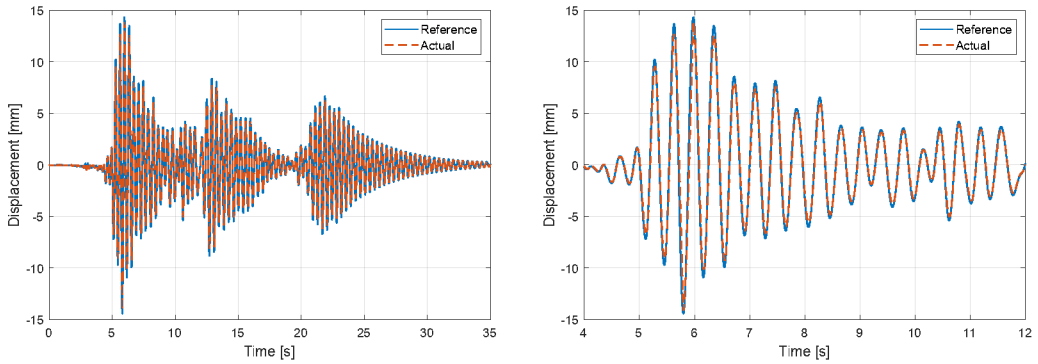

Figure 8. Comparison between reference and actual position of the shaker for uncontrolled building (40% Irpinia earthquake): overall time history (a) and detail time history (b).

Table 3. Comparison between the Reference and Actual displacement for different tests

Test	Seism Intensity	Max Reference Displacement	Max Actual Displacement	Delta Error
#1	10%	2.005 mm	1.922 mm	4.11%
#2	10%	2.005 mm	1.904 mm	5.03%
#3	40%	14.41 mm	14.07 mm	2.36%
#4	40%	14.41 mm	14.09 mm	2.15%

Once the HIL's performances had been proved, the next step was to evaluate the effectiveness of the AMD in reducing the building's oscillations.

4.1 Sky-Hook Control Tuning

For the vibration control algorithm, we studied the two different conditions: fully-infilled structure and bare-frame structure. Respectively, these represent the initial state of the building in the seismic event and the final one if damage to non-structural elements occurred. It is important to clarify that a study of the analytical building model with structural damage should not be necessary, since this would mean failure of the AMD. However, proper control strategies can be implemented even for this critical scenario with the aim of autonomously adopting the correct control gain.

Starting from these considerations, the Sky-Hook damping coefficient was set to obtain good control performance preserving the stability of the control system in every condition. For this reason, a study of the Root Locus (RL) control system was performed. The RL shown in Figure 9 represents the first 3 complex conjugate poles of the structure, for the fully-infilled model and the bare-frame one respectively, varying the control parameter G. The Sky-Hook damping values were changed within a range between $G = 0$ (green square), corresponding to the uncontrolled structure, and $G = 2 \cdot 10^6$ (red star), corresponding to the "critical" controlled condition.

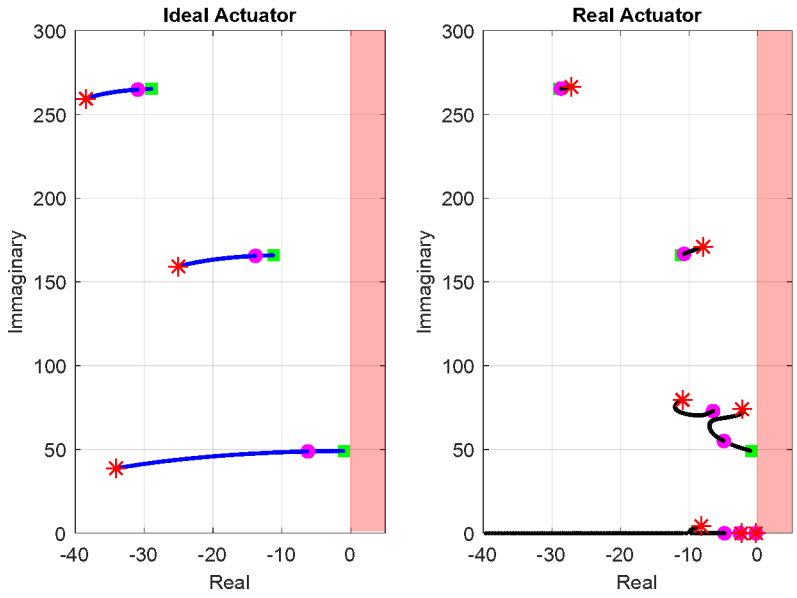

(a)

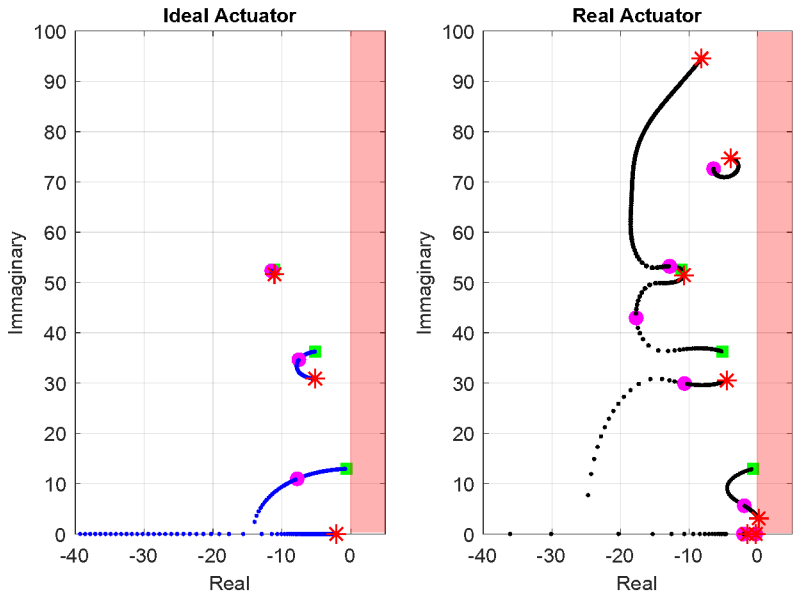

(b)

Figure 9. R-Locus of the Infilled (a) and Bare-Frame (b) Structure for different values of Sky-Hook coefficient: the green square represents the uncontrolled building, the purple circle represents the controlled one with tuned gain, the red star represents the controlled building with a "too-high" gain.

Indeed, in the case of an ideal actuator, which cannot introduce delay or magnitude amplification, the building's damping increases proportionally with the gain, never leading to system instability. Unfortunately, accounting for the real actuator dynamics, on increasing G over a certain threshold, we obtain a reduction of the overall damping that could eventually lead to instability (see, for example, the

red star in Figure 9b). Thus, in order to obtain a robust control, we selected a Sky-Hook gain (purple circle) equal to $3.5 \cdot 10^5$, which is near the optimum in both the cases.

Table 4 quantifies the overall structural damping variation, for the 3 control gains for both the infilled and bare-frame building. For Sky-Hook gain values that are too high (red stars), the overall structural damping decreases to instability. The selected "optimal" gain (purple circle) introduces a significant increment of the damping, avoiding instability with a good safety margin.

Table 4. The overall structural damping for the controlled structures (fully-infilled and bare-frame) for different Sky-Hook control gains

Structure	Sky-Hook Gain	ξ_1	ξ_2	ξ_3
Fully-Infilled	***null***	2.0%	6.8%	10.9%
	optimal	8.9%	6.5%	10.8%
	too high	3.1%	4.6%	10.2%
Bare-Frame	***null***	5.0%	14.3%	21.2%
	optimal	39.4%	42.4%	23.1%
	too high	unstable	20.9%	8.7%

The increase in damping is especially high for the first vibration mode, mainly associated with large displacements responsible for damage during a seismic event (the earthquake's low-frequency contribution).

4.2 Experimental Results

After the tuning procedure, many tests were conducted in order to prove the performance of the I-Pro 1. For the sake of simplicity, only the most significant results are reported here.

First, the AMD reference force tracking was analysed. The same test, done previously to evaluate the HIL's performance, was repeated activating the I-Pro 1. In Figure 10 time histories of ~~comparison between~~ the reference force and the actual force, computed by the measurements of the accelerometer placed on the moving mass, are shown, while in Table 5 their maximum values reached during different tests are reported. The good match between reference force and actual force generated demonstrates the effectiveness of AMD force control logic.

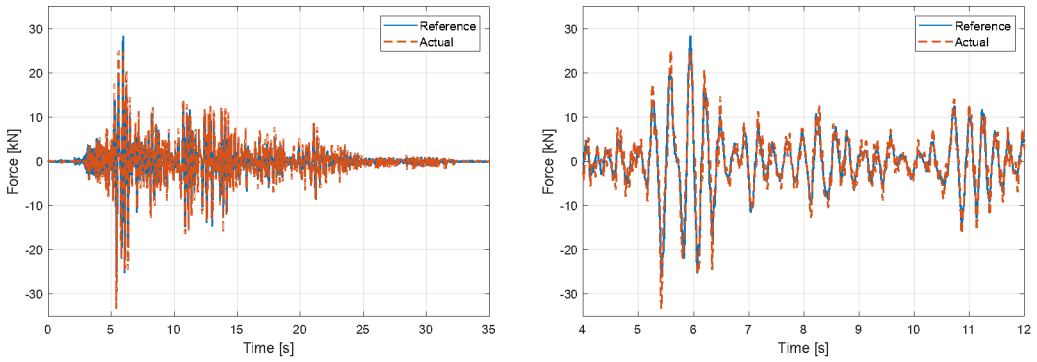

Figure 10. Comparison between reference and actual force of the AMD for controlled structure (40% Irpinia earthquake): overall time history (a) and detail time history (b).

Table 5. Comparison between the Reference and Actual force for different simulation

Test	Seism Intensity	Max Reference Force	Max Actual Force	Delta Error
#1	10%	6.61 kN	6.93 kN	4.87%
#2	40%	28.28 kN	31.57 kN	11.60%
#3	40%	26.23 kN	28.63 kN	9.16%

Then, the I-Pro 1's ability to protect a building against an earthquake was investigated. A comparison between controlled and uncontrolled structure rooftop displacement was done, varying the earthquake intensity and the target overall structural damping. In Figure 11 the time histories of the roof's displacement with the optimal control tuning are depicted, for the 10% and the 40% of the Irpinia seismic event respectively, comparing the controlled and the non-controlled cases. Table 6 shows the maximum roof displacement reached during the seismic event for different intensities of earthquake magnitude and different control gains.

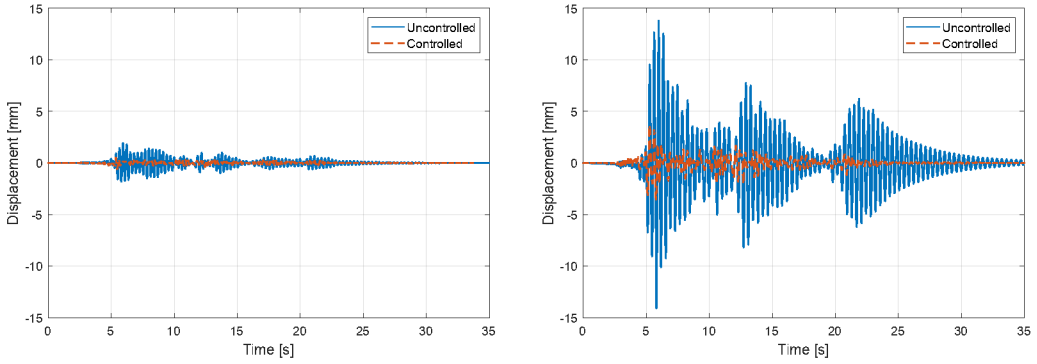

Figure 11. Roof displacement time history: comparison between the uncontrolled and the controlled building response, for a ground intensity of 10% (a) and 40% (b) of the Irpinia earthquake.

Table 6. Maximum Roof Displacement: comparison between the uncontrolled building (NC) and the controlled one (C)

Test	Seism Intensity	ξ_1	NC Roof Displacement	C Roof Displacement	Reduction
#1	10%	7.3%	1.92 mm	1.01 mm	47.24%
#2	10%	8.9%	1.92 mm	0.58 mm	68.85%
#3	40%	7.3%	14.07 mm	4.99 mm	64.49%
#4	40%	8.5%	14.07 mm	3.92 mm	72.11%
#5	40%	8.9%	14.07 mm	3.69 mm	73.71%

One can see that the displacement reduction increases with the earthquake's intensity and the target overall damping. This is due to the implementation of a non-linear structural model. Indeed, a higher seismic magnitude (40%) generates greater damage in the uncontrolled building, that modifies its dynamics from an infilled to a bare-frame structure. On the contrary, in the controlled case, the lower displacements make it possible to preserve the infilled structure and maintain a greater building stiffness.

5 Conclusion

In this work, a novel procedure for the validation and testing of an Active Mass Damper system for seismic applications is presented. The device adopted as a test case is the ISAAC I-Pro 1, a hydraulic AMD able to generate peak linear forces of up to 220 kN with a moving mass of 2200 kg.

The control scheme of the AMD was presented in detail, from position control of the moving mass to the high-level vibration control logic designed to protect the building in case of seismic events. For the latter a Sky-Hook control logic was adopted, proving to be a simple tuning procedure with good performance in vibration suppression for the two limit conditions: fully-infilled structure and bare-frame structure.

The AMD selected was investigated on a dedicated HIL test bench. The HIL architecture made it possible to simulate the real response on the rooftop of a 3-storey building subjected to a real seismic event (the Irpinia 1980 earthquake), numerically computed and reproduced by means of the actuated shaking table. The loop was closed by the control force generated by the AMD and estimated by means of an accelerometer placed on the moving mass. The delay introduced by the shaking table was balanced by adopting a TVC control logic and a stability analysis of the combined system (HIL and AMD) was performed.

The HIL architecture proposed was successfully adopted to test the performance of the proposed hydraulic AMD. In particular, the tests performed made it possible to validate:

- The ability of the HIL architecture to reproduce the oscillations of the building's rooftop, including the non-linear effects due to ongoing damage to the structure
- The AMD's effectiveness in reducing the oscillations of the building subjected to an input seismic action

- The robustness of the proposed control logic.

Declaration of conflicting interests

The author(s) declared no potential conflicts of interest with respect to the research, authorship, and/or publication of this article.

Funding

The author(s) received no financial support for the research, authorship, and/or publication of this article.

References

[1] Aiqun Li (2020) Vibration Control for Building Structures, Theory and Applications. Springer.

[2] Beards CF (1996) Structural Vibration. *Butterworth-Heinemann*.

[3] Bolt BA (2020) Earthquake. *Encyclopædia Britannica*.

[4] Bui H-L, Nguyen C-H, Bui V-B, Le K-N and Tran H-Q (2017) Vibration control of uncertain structures with actuator saturation using hedge-algebras-based fuzzy controller. *Journal of Vibration and Control* 23(12): 1984-2002.

[5] Calvi Paolo M and Calvi Gian Michele (2018) Historical development of friction-based seismic isolation systems. *Soil Dynamics and Earthquake Engineering* 106: 14-30.

[6] Cavaleri L., Di Trapani F. (2014) Cyclic response of masonry infilled RC frames: Experimental results and simplified modeling. *Soil Dynamics and Earthquake Engineering*

[7] Cheng FY, Jiang Hongping, and Lou Kangyu (2008) Smart structures: innovative systems for seismic response control. *CRC Press*.

[8] Fahy F and Gardonio P (2007) Sound and Structural Vibration. *Academic Press*.

[9] Guclu R and Yazici H (2007) Fuzzy Logic Control of a Non-linear Structural System against Earthquake Induced Vibration. *Journal of Vibration and Control* 13(11): 1535-1551.

[10] Gutierrez SM and Adeli H (2013) Tuned Mass Dampers. *Archives of Computational Methods in Engineering*. 20(4): 419–431.

[11] Hak S., Morandi P., Magenes G. & Sullivan T.J. (2012) Damage Control for Clay Masonry Infills in the Design of RC Frame Structures. *Journal of Earthquake Engineering*

[12] Ikeda Y, Sasaki K, Sakamoto M and Kobori T (2001) Active mass driver system as the first application of active structural control. *Earthquake Engineering and Structural Dynamics*

[13] Madan Alok (2005) Vibration control of building structures using self-organizing and self-learning neural networks. *Journal of Sound and Vibration* 287: 759-784.

[14] Matsumoto Y, Hasegawa O, Shimoda I and Seto K (2004) Fundamental study of Active Mass Damper for improving livability against traffic vibration. *Seismic Engineering*

[15] Miyazaki M, Ikenaga M and Fujita T (2004) Fundamental study of active mass damper for slender houses. *13th World Conference on Earthquake Engineering* 732.

[16] Ning D, Du H, Sun S, Zheng M, Li W, Zhang N and Jia Z (2020) An Electromagnetic Variable Stiffness Device for Semiactive Seat Suspension Vibration Control. *IEEE Transactions on Industrial Electronics* 67(8): 6773-6784.

[17] Jue Wang, Fujiang Jin, Lichun Zhou and Ping Li (2019) Implementation of model-free motion control for active suspension systems. *Mechanical Systems and Signal Processing* 119: 589-602.

[18] Patil SJ and Reddy GR (2012) State of Art Review - Base Isolation Systems for Structures. *International Journal of Emerging Technology and Advanced Engineering* 2(7): 438-453.

[19] Rahmi Guclu (2006) Sliding mode and PID control of a structural system against earthquake. *Mathematical and Computer Modelling* 44 (1–2): 210-217.

[20] Sakizlis V, Kakalis NMP, Dua V, Perkins JD and Pistikopoulos EN (2004) Design of robust model-based controllers via parametric programming. *Automatica* 40(2): 189-201.

[21] Septimiu Luca, Florentina Chira and Roşca V-O (2005) Passive, Active and Semi-Active Control Systems in Civil Engineering. *Bulletin of the Polytechnic Institute of Jassy* 3-4: 23-32.

[22] Shen G, Zheng ST, Ye ZM, Yang ZD, Zhao Y and Han JW (2011) Tracking control of an electro-hydraulic shaking table system using a combined feedforward inverse model and adaptive inverse control for real-time testing. *Proceedings of the Institution of Mechanical Engineers, Part I: Journal of Systems and Control Engineering* 225(5): 647-666.

[23] Snoonian D (2003) Smart buildings. *IEEE Spectrum* 40(8): 18-23.

[24] Tait MJ, Isyumov N. and El Damatty AA (2008) Performance of Tuned Liquid Dampers. *Journal of Engineering Mechanics* 134(5): 417-427.

[25] Thenozhi S and Yu W (2015) Active vibration control of building structures using fuzzy proportional-derivative/proportional-integral-derivative control. *Journal of Vibration and Control* 21(12): 2340-2359.

[26] Ubertini F, Venanzi I and Comanducci G (2015) Considerations on the implementation and modeling of an active mass driver with electric torsional servomotor. *Mechanical Systems and Signal Processing* 58-59: 53-69.

[27] Xu H, Zhang C, Li H and Ou J (2014) Real-time hybrid simulation approach for performance validation of structural active control systems: a linear motor actuator based active mass driver case study. *Structural Control and Health Monitoring* 21: 574-589.

[28] Yamamoto M, Aizawa S, Higashino M and Toyama K (2001) Practical applications of active mass dampers with hydraulic actuator. *Earthquake Engineering & Structural Dynamics* 30(11): 1697-1717.

[29] Yang SM, Chen CJ and Huang WL (2006) Structural Vibration Suppression by a Neural-Network Controller with a Mass-Damper Actuator. *Journal of Vibration and Control* 12(5): 495-508.

[30] Yang JN, Wu JC, Agrawal AK and Hsu SY (1997) Sliding mode control with compensator for wind and seismic response control. *Earthquake Engineering and Structural Dynamics* 26 (11): 1137-1156.

[31] Yu T, Zhencai Z, Gang S and Xiang L (2015) Experimental investigation of feedforward inverse control with disturbance observer for acceleration tracking of electro-hydraulic shake table. *Journal of Vibroengineering* 17(1): 330-345.

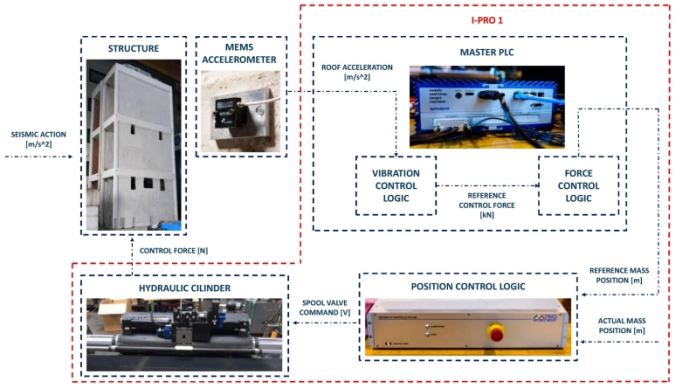

Figure 1. Block diagram of the ISAAC I-PRO1 Control Algorithm.

209x296mm (300 x 300 DPI)

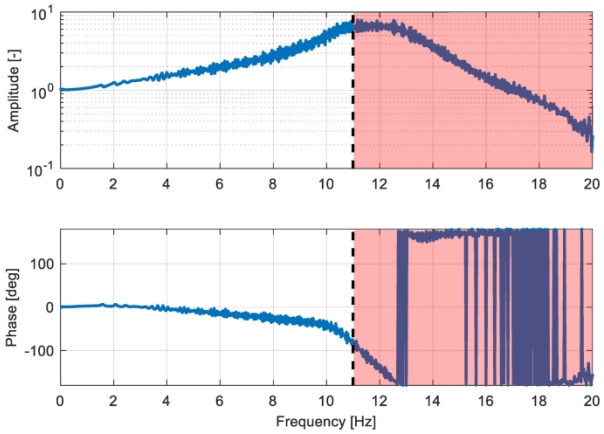

Figure 2. The position control logic: Frequency Response Function (FRF) between actual and reference position.

209x296mm (300 x 300 DPI)

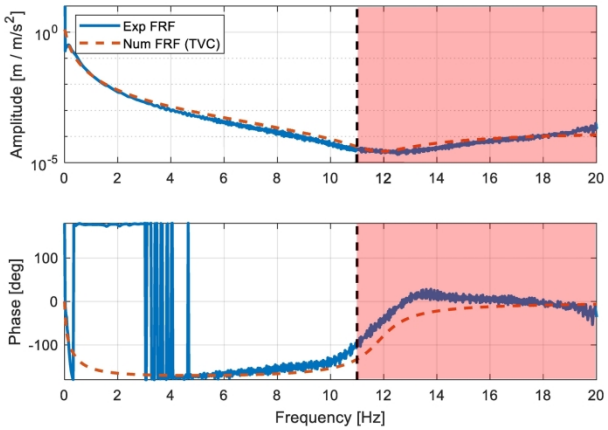

Figure 3. The force control logic: comparison between the experimental and the numerical-TVC FRF (between acceleration and position of the AMD moving mass).

209x296mm (300 x 300 DPI)

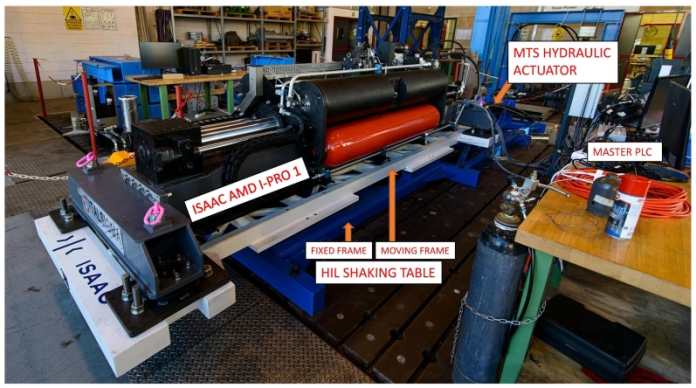

Figure 4. Overall view of the physical HIL system.

209x296mm (300 x 300 DPI)

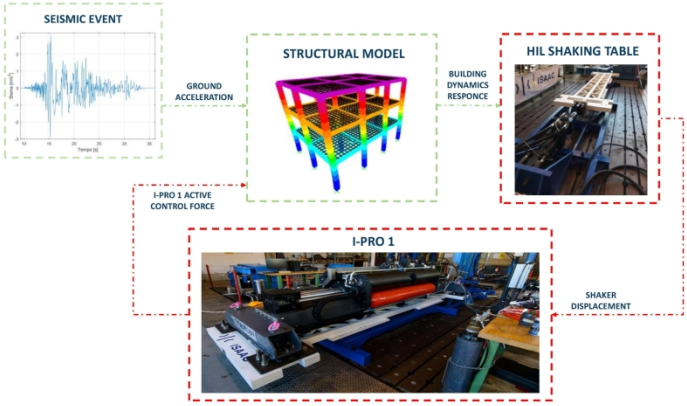

Figure 5. Hardware in the Loop (HIL) scheme: physical (red lines) and virtual (green lines) signals.

209x296mm (300 x 300 DPI)

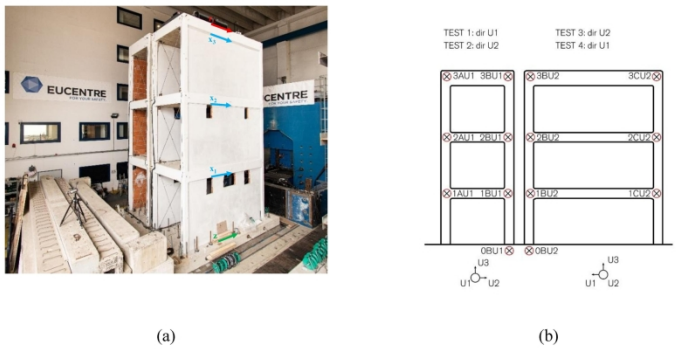

(a) (b)

Figure 6. The full scale real three-storey building placed in the EUCENTRE Laboratory (a) and Experimental Modal Analysis (EMA) on the 3-story RC building: layout of the sensors and summary of the test performed (b).

209x296mm (300 x 300 DPI)

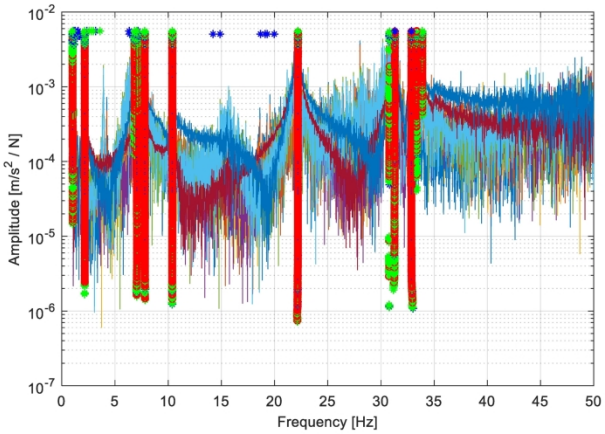

Figure 7. Example of PolyMAX Stability diagram calculated during the Experimental Modal Analysis (EMA) on the fully-infilled structure. FRFs between the accelerations measured at different points of the structure and the force of the vibrodine placed on the top floor.

209x296mm (300 x 300 DPI)

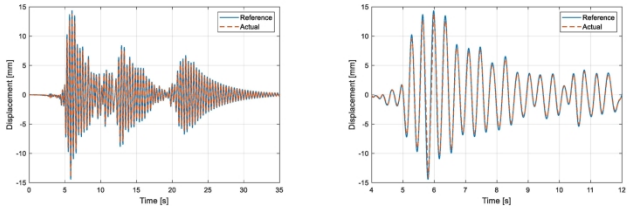

Figure 8. Comparison between reference and actual position of the shaker for uncontrolled building (40% Irpinia earthquake): overall time history (a) and detail time history (b).

209x296mm (300 x 300 DPI)

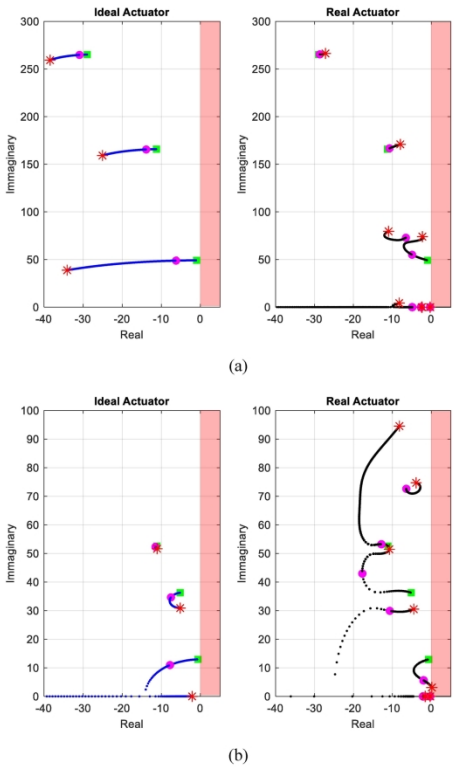

Figure 9. R-Locus of the Infilled (a) and Bare-Frame (b) Structure for different values of Sky-Hook coefficient: the green square represents the uncontrolled building, the purple circle represents the controlled one with tuned gain, the red star represents the controlled building with a "too-high" gain.

209x296mm (300 x 300 DPI)

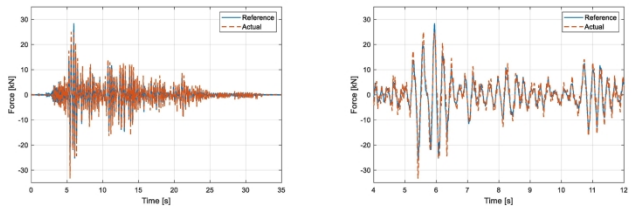

Figure 10. Comparison between reference and actual force of the AMD for controlled structure (40% Irpinia earthquake): overall time history (a) and detail time history (b).

209x296mm (300 x 300 DPI)

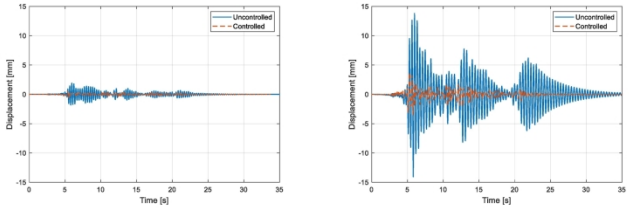

Figure 11. Roof displacement time history: comparison between the uncontrolled and the controlled building response, for a ground intensity of 10% (a) and 40% (b) of the Irpinia earthquake.

209x296mm (300 x 300 DPI)